

# Final state interactions in electron scattering at high missing energies and momenta

C. Barbieri<sup>a,b,\*†</sup>

<sup>a</sup>TRIUMF, 4004 Wesbrook Mall, Vancouver, British Columbia, Canada V6T 2A3

<sup>b</sup>Gesellschaft für Schwerionenforschung, Planckstr. 1, 64291, Darmstadt, Germany

Calculations of two-step rescattering and pion emission for the  $^{12}\text{C}(e, e'p)$  reaction at very large missing energies and momenta are compared with recent data from TJNAF. For parallel kinematics, final state interactions are strongly reduced by kinematical constraints. A good agreement between calculation and experiment is found for this kinematics when one admits the presence of high momentum components in the nuclear wave function.

*Key words:* electron scattering, short range correlations  
*PACS:* 25.30.Fj, 25.30.Dh, 21.60.-n, 21.10.Pc, 21.10.Jx.

In recent years, electron scattering experiments have been possible with kinematics that involve large energies and momentum transfered, as for example in studies of nuclear transparency. In this regime, the final state interactions (FSI) for the knock out of a nucleon are usually treated employing Glauber inspired calculations [1,2,3,4]. Such techniques, together with the experience gained in related nuclear structure studies, provide a useful starting point to pursue accurate predictions of neutrino-nucleus interactions at high energy. This was pointed out by various contributions to this conference.

At scattering energies of the order of GeV, the leptonic probe can resolve the high-momentum tail of the spectral function generated by short-range (central and tensor) correlations (SRC). This represent about 10-20% of the total spectral strength [5,6] and is found along a ridge in the momentum-energy plane ( $k$ - $E$ ) which spans a region of several hundred MeV/c (MeV) [7,9,8]. This corresponds to large missing momenta ( $p_m$ ) and energies ( $E_m$ ) in knock out cross sections. This contribution to the spectral function is also responsible for most of the binding energy of nuclear systems [10]. The main characteristics pre-

dicted by these calculations are confirmed by recent experimental data [11,12,13], which will be considered further below.

Locating this strength experimentally, at both large  $E_m$  and  $p_m$ , is difficult because it is spread over an energy range of several hundred MeV, so the total density of the spectral function is very low. In this energy regime multi-nucleon processes, beyond the direct knock out, are possible [14] and can induce large shifts in the missing energies and momenta, moving strength to regions where the direct signal is much smaller and therefore submerging it. As it will be discussed below, the effects of FSI become larger and less controllable when the transverse structure functions that enter the expression of the  $(e, e'p)$  cross section dominate the longitudinal one. This trend is predicted by several theoretical studies [14,15,16,17,18]. The issue of how to control FSI in lepton scattering experiments has been discussed in detail in Ref. [19,20] for the particular case of kinematics sensitive to the SRC tail of the nuclear spectral function. A Monte Carlo simulation and kinematical arguments led to the suggestion that the best chance for an identification of SRC occurs in parallel kinematics <sup>3</sup>.

\*Email: C.Barbieri@gsi.de

<sup>†</sup>Present address: Gesellschaft für Schwerionenforschung, Planckstr. 1, 64291, Darmstadt, Germany

<sup>3</sup>In this work we refer to 'parallel' and 'perpendicular' kinematics in terms of the angle between the momentum transferred by the leptonic current  $\mathbf{q}$  and the momentum of

The latter also tend to be less sensitive to meson exchange currents (MEC) – which involve transverse excitations – and are cleaner due to the high momentum that is required for the detected proton. New data were subsequently taken by the E97-006 collaboration at Jefferson Lab [21,11,12] for a set of nuclei ranging from carbon to gold. Both optimal (parallel) and perpendicular kinematics were used, to provide useful data for investigating the reaction mechanism.

At the energy regime of the JLab experiment, the main contribution to FSI, below the meson production threshold, is identified with two-step rescattering. This has been studied recently in Refs. [22,23] using a semiclassical model, which has the advantage of describing the distortion due to FSI in terms of the full one-hole spectral function. This accounts for both the momentum and the energy distribution of the original correlated strength, which is of importance for the proper description of the response [24]. In this letter we extend the analysis of Ref. [23] by including the contributions of  $\pi$ -emission and compare with the data of Ref. [21].

In the ideal case where only the direct knock out process was relevant, the  $(e, e'p)$  cross section for emitting a proton from a nucleus with spectral function  $S_p^h(k, E)$  would be correctly described by plane wave impulse approximation (PWIA),

$$\frac{d^6\sigma_{PWIA}}{dE_0 d\Omega_{\hat{k}_o} dE_f d\Omega_{\hat{p}_f}} = |\mathbf{p}_f| E_a S_a^h(|\mathbf{q} - \mathbf{p}_f|, \omega - E_f) \sigma_{ea}^{cc} \mathcal{T}, \quad (1)$$

where  $(E_o, \mathbf{k}_o)$ ,  $(E_f, \mathbf{p}_f)$  and  $(\omega, \mathbf{q})$  represent the four-momenta of the detected electron, the final proton and the virtual photon, respectively.  $\sigma_{eN}^{cc}$  is the electron-nucleon cross section. The present calculations employed the  $\sigma^{cc}$  prescription discussed in Ref. [21], which is obtained by using the on-shell current also for off-shell protons<sup>4</sup>. In

the initial nucleon  $\mathbf{p}_i = -\mathbf{p}_m$  (as opposed to the detected proton  $\mathbf{p}_f$ ). This definition is more restrictive in the limit of high momentum transfer, where  $\mathbf{q}$  and  $\mathbf{p}_f$  tend to be collinear anyhow.

<sup>4</sup>Preferably one uses a prescription to extrapolate the on-shell cross section to the off-shell case while preserving energy and current conservation. The analysis of several possible prescriptions carried out in Ref. [21] found that

Eq. (1), the transparency factor  $\mathcal{T}$  accounts for the loss of flux from the direct channel due to the FSI [4]. However, one still has to correct for the reappearance of strength through other reaction channels.

In Ref. [23], we considered the two-step mechanism where the knock out reaction  $(e, e'a)$  for a nucleon  $a$  is followed by a scattering process from another nucleon in the medium,  $N'(a, p)N''$ . Eventually, leading to the emission of the detected proton and an undetected nucleon  $N''$ . Three channels are possible, in which  $a$  represents either a proton (with  $N' = p$  or  $n$ ) or a neutron (with  $N' = p$ ). The semi-exclusive cross section for these events was calculated semiclassically as [22]

$$\begin{aligned} & \frac{d^6\sigma_{rescatt.}}{dE_0 d\Omega_{\hat{k}_o} dE_f d\Omega_{\hat{p}_f}} \\ &= \sum_{a, N'=1,2,3} \int d\mathbf{r}_1 \int d\mathbf{r}_2 \int_0^\omega dT_a \rho_N(\mathbf{r}_1) \\ & \times \frac{|\mathbf{p}_a| E_a S_a^h(|\mathbf{q} - \mathbf{p}_a|, \omega - E_a) \sigma_{ea}^{cc}}{M (\mathbf{r}_1 - \mathbf{r}_2)^2} \\ & \times g_{aN'}(|\mathbf{r}_1 - \mathbf{r}_2|) P_T(p_a; \mathbf{r}_1, \mathbf{r}_2) \rho_{N'}(\mathbf{r}_2) \\ & \times \frac{d^3\sigma_{aN'}}{dE_f d\Omega_{\hat{p}_f}} P_T(p_f; \mathbf{r}_2, \infty). \end{aligned} \quad (2)$$

Eq. (2) assumes that the intermediate particle  $a$  is generated in (PWIA) by the electromagnetic current at a point  $\mathbf{r}_1$  inside the nucleus. Here,  $S_a^h(k, E)/M$  is the spectral function of the hit particle  $a$  normalized to one [i.e.,  $M = N(Z)$  if  $a$  is a neutron (proton)]. The pair distribution functions  $g_{aN'}(|\mathbf{r}_1 - \mathbf{r}_2|)$  account for the joint probability of finding a nucleon  $N'$  at  $\mathbf{r}_2$  after the particle  $a$  has been struck at  $\mathbf{r}_1$  [26]. The kinetic energy  $T_a$  of the intermediate nucleon  $a$  ranges from 0 to the energy  $\omega$  transferred by the electron. The point nucleon densities  $\rho_N(\mathbf{r})$  were derived from experimental charge distributions by unfolding the proton size [27]. The factor  $P_T(p; \mathbf{r}_1, \mathbf{r}_2)$  gives the transmission probability that the struck particle  $a$  propagates, without any interactions,

the best agreement between the data of different kinematics is obtained by avoiding any of the *ad hoc* modifications of the kinematics at the electromagnetic vertex as suggested in Ref. [25].

to a second point  $\mathbf{r}_2$ . There, it rescatters from the nucleon  $N'$  with cross section  $d^3\sigma_{aN'}$ .

The second contribution to the  $(e, e'p)$  cross section considered here is the production of an undetected pion. By following a PWIA approach this can be written as

$$\begin{aligned} \frac{d^6\sigma_{\pi emiss.}}{dE_0 d\Omega_{\hat{k}_o} dE_f d\Omega_{\hat{p}_f}} &= \Gamma_v \sum_{a=p,n} \mathcal{T} \\ &\times \int d\mathbf{k}_\pi \frac{W^2 |\mathbf{p}_f|}{(\omega - E_f - \omega_\pi) \omega_\pi k_\gamma} S_a^h(|\mathbf{p}_b|, E_b) \\ &\times [R_T^a + \varepsilon_L R_L^a + \varepsilon \cos(2\phi) R_{TT}^a + \\ &+ \sqrt{2\varepsilon_L(1+\varepsilon)} \cos(\phi) R_{LT}^a] , \end{aligned} \quad (3)$$

where,  $(\omega_\pi, \mathbf{k}_\pi)$  represent the four-momenta of the emitted pion,  $W$  is the invariant mass of the emitted pion-nucleus pair,  $\Gamma_v = (\alpha k_\gamma k_o)/[2\pi k_i Q^2(1-\varepsilon)]$  is the flux of virtual photon field [28] and the momentum and energy of the bound nucleon are  $\mathbf{p}_b = \mathbf{q} - \mathbf{p}_f - \mathbf{k}_\pi$  and  $E_b = \omega - T_f - T_\pi - T_{rec}$ . The response functions  $R_{xy}^a$  refer to the production of a  $\pi^0$  ( $\pi^-$ ) when the struck nucleon  $a$  is a proton (neutron). In the spirit of the PWIA approach, we employed response functions for pion production on a free nucleon, evaluated using the MAID program [29,30]. These depend on  $W$  and the angle  $\phi$  between the pion and the photon in the c.o.m. frame.

Recently, the experimental strength measured for  $^{12}\text{C}$  in parallel kinematics was compared to theory [11,12]. For missing energies up to 200 MeV, the summed strength measured turned out to agree with theoretical predictions. Moreover, the ridge-like shape of strength distribution was observed except that the position of the peak was found at lower missing energies than predicted by theory. At the same time, Eq. (2) predicts little or negligible effects from FSI in the region of the comparison (see Ref. [22] and discussion of Fig. 1 below). This gives confidence that, for the first time, effects of the high momentum components attributed to SRC could be observed without being overwhelmed by the distortion of FSI. However, a quantitative understanding of the reaction mechanism is still needed.

In order to make a meaningful comparison be-

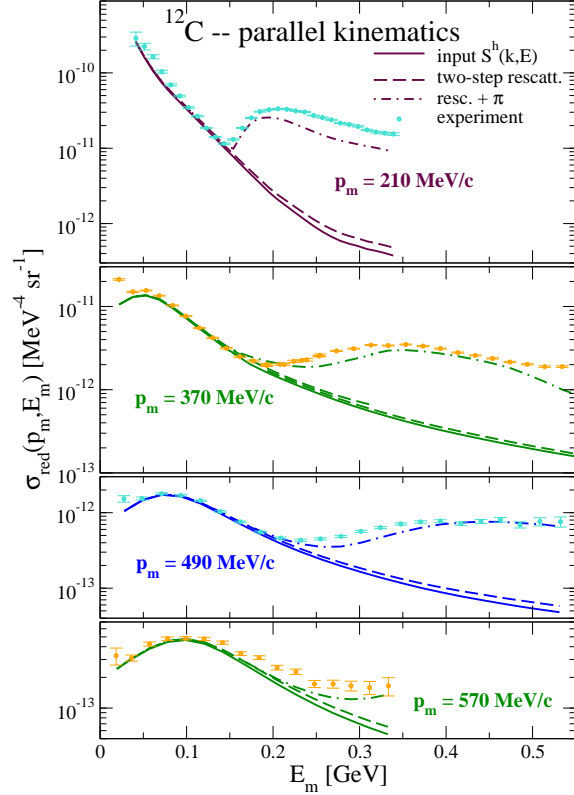


Figure 1. (Color online) Theoretical results for the reduced cross section of  $^{12}\text{C}$  obtained in parallel kinematics compared with the experimental results of Ref. [21]. The full line shows the model spectral function, Eq. (4), employed in the calculations. The dashed lines include the additional effects of rescattering, Eq. (2), while the combined prediction of Eq. (1–3) is given by the dot-dashed lines.

tween the experiment and the theoretical predictions for FSI, one needs a proper ansatz for the undistorted spectral function,  $S^h(k, E)$  in Eqs. (2) and (3). At low energies and momenta we employed the correlated part of the spectral function  $S_{LDA}^h(k, E)$  in Ref. [8] which was obtained using local density approximation (LDA), and combined it with a properly scaled spectral

function  $S^h_{WS}(k, E)$  derived from an adequate Wood–Saxon potential. This includes the bulk of the spectral strength, located in the mean field (MF) region up to a momentum of  $\approx 250$  MeV/c. The remaining strength is located along the SRC ridge. This represents only a fraction of the total number of nucleons in the system but it is the part probed by the kinematics under consideration. Thus, the most important for the present analysis. As stated above, theoretical calculations can reproduce the qualitative shape of this distribution and the total summed strength but miss the position peak [12]. As we are mainly interested in the reaction mechanism, it is preferable to parameterize the SRC part of the input spectral function in terms of a Lorentzian energy distribution, which was fitted to the experimental results for  $^{12}\text{C}$  in parallel kinematics [23]. The full spectral function employed in Eqs. (1–3) is [23]

$$S^h(k, E) = \begin{cases} S^h_{Lorentzian}(k, E) & \text{for } k > 230 \text{ MeV/c} \\ & \text{and } E > 19 \text{ MeV,} \\ S^h_{LDA+WS}(k, E) & \text{otherwise.} \end{cases} \quad (4)$$

In the following, we compare the predictions of the above model to the experimental data in regions far from the correlated peak and in different kinematics.

Figure 1 compares the results obtained in parallel kinematics to the experimental reduced cross section defined as  $\sigma_{red}(p_m, E_m) = \sigma_{experiment} / (|p_f E_f| \sigma_{ep}^{cc} \mathcal{T})$ . When only the PWIA contribution, Eq. (1), is included (full line) one compares the experiment to the assumed input spectral function  $S^h(k, E)$ , showing the quality of the fit around the correlated peak. It is also seen that the contribution from rescattering processes (dashed line) is negligible in this region and increases only at very large missing energies [22]. Thus, validating the choice of taking the input spectral function in this region from the experiment. It is important to observe that the main reason for the small effects of rescattering obtained in this calculation is kinematical in origin. Due to rescattering events, the emitted nucleon loses part of its initial energy by knocking out a second particle. The requirement of small angles between the momenta  $\mathbf{q}$  and  $\mathbf{p}_i$  implies larger en-

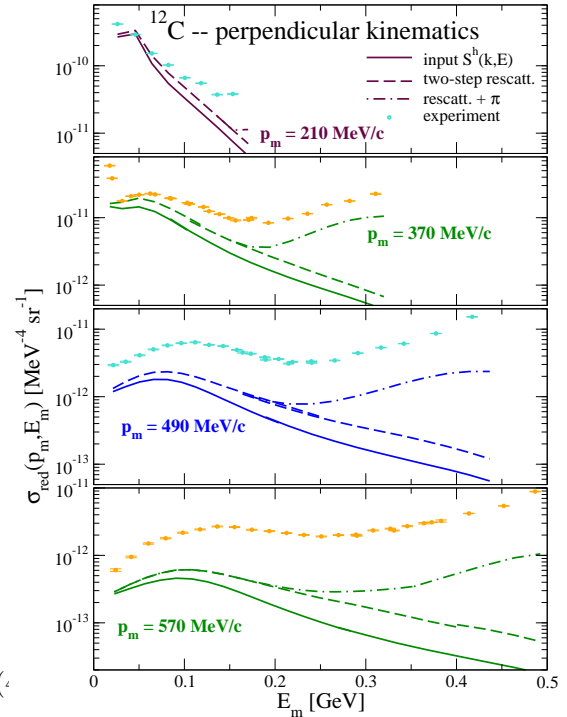


Figure 2. (Color online) Theoretical results for the reduced cross section of  $^{12}\text{C}$  obtained in perpendicular kinematics compared with the experimental results of Ref. [21]. The full line shows the model spectral function, Eq. (4), employed in the calculations. The dashed lines include the additional effects of rescattering, Eq. (2), while the combined prediction of Eq. (1–3) is given by the dot-dashed lines.

ergies  $T_a$  (i.e. smaller  $E_m$ ) and larger missing momenta for the intermediate nucleon, with respect to the detected proton. This forces sampling the rescattered strength in regions where the correlated spectral function is smaller than for the direct process. For analogous reasons, multiple rescattering effects become even less important, as seen in Ref. [15] for perfectly parallel kinematics. Sensible deviation from the Lorentzian shape of the peak are observed once the pion emission

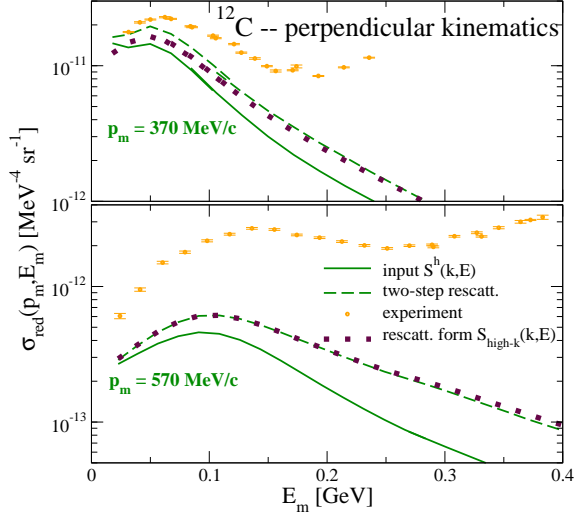


Figure 3. (Color online) Rescattering contribution to the reduced cross section for  $^{12}\text{C}$  in perpendicular kinematics (dashed line). The dotted lines show the analogous results obtained by neglecting the rescattering from the MF region,  $S_{LDA+WS}^h(k, E)$ , in Eq. (4). The full line shows the model spectral function, Eq. (4), employed in the calculations and the experimental data are from Ref. [21]

threshold is reached. Then, a distorted image of the correlated region is produced at larger missing energies (due to the extra energy necessary to create the pion). The nice agreement between the total theoretical cross section and the experiment confirms that in parallel kinematics the contribution of FSI becomes relevant only at large missing energies and it is dominated by  $(e, e'p\pi)$  events. As the missing momentum increases, the regions dominated by correlated nucleons and pion production tend to overlap. We note that as long as multiple rescattering effects can be neglected no sensible quantum interference effect is expected, since Eqs. (1–3) lead to different particles in their final states.

The experimental data are found to be sensibly larger in perpendicular kinematics than in paral-

lel ones [21]. These are compared with the results of Eqs. (2-3) in Fig. 2. In this case, the rescattered strength is large and affects the reduced spectral function already at the top of the SRC tail. Due to the much larger redistribution of spectral strength the valley between the SRC and meson production regions is also filled in and it is no longer possible to distinguish them. The combined predictions of single rescattering and pion emission are able to reproduce the shape of the measured cross section but results in sensibly lower cross sections. Fig. 2 shows that Eq. (2) can account for the differences between parallel and perpendicular kinematics for  $E_m \approx 50$  MeV and  $p_m < 350$  MeV/c. However, the experiment is strongly under predicted over most of the correlated region. For  $p_m = 570$  MeV/c, the cross section is predicted to be 50% larger than the direct process, whereas the experiment is almost of one order of magnitude above. We conclude that two-step rescattering represents only a fraction of the total FSI present in perpendicular kinematics. A possible contribution that could bring theory and data closer together is that of MEC that involve the excitation of a  $\Delta$  or higher resonances. These are known to be sensitive to transverse degrees of freedom.

We observe that the larger contribution of Eq. (2) with respect to parallel kinematics can also be understood kinematically. In this case a nucleon can lose energy in a rescattering event but still be detected with a missing momentum larger than its initial momentum. This results in moving strength from regions where the spectral function is large to regions where it is small, thereby submerging the direct signal. The shift is large enough that measurements in the correlated region can be affected by events originating from MF orbits [22]. The size of this effect for two-step rescattering is however limited to the part of the correlated region at low missing momenta. This is shown in Fig. 3, where the dotted lines have been obtained by setting  $S_{LDA+WS}^h(k, E) = 0$  in Eq. (4). Single rescattering from the MF strength gives no appreciable contribution at missing momenta above 500 MeV/c. For parallel kinematics a similar comparison shows no visible effects at even lower momenta, indicating that rescattering

moves strength *only* within the correlated region itself. This supports the necessity of including the observed high momentum strength already in  $S^h(k, E)$ , that is, in the nuclear wave function.

In conclusion, first predictions of two-step rescattering and pion emission in  $(e, e'p)$  reactions at large  $p_m$ - $E_m$  were discussed and compared to experimental data [21,11]. The results are understood in terms of kinematical constraints and confirm the expectation that, for light nuclei and properly chosen parallel kinematics, the effects of FSI can be small for missing energies up to the  $\pi$  production threshold. In perpendicular kinematics the agreement between data and theory is less favorable. This suggests that additional ingredients of transverse character, such as MEC, should be investigated in future calculations.

Several illuminating discussions with D. Rohe, I. Sick and L. Lapikás are acknowledged. This work was supported by the Natural Sciences and Engineering Research Council of Canada (NSERC).

## REFERENCES

1. C. Ciofi degli Atti and L. Kaptari, Phys. Rev. C **71**, 024005 (2005).
2. M. M. Sargsian, T. V. Abrahamyan, M. I. Strikman and L. L. Frankfurt, Phys. Rev. C **71**, 044614 (2005).
3. R. Schiavilla, O. Benhar, and A. Kievsky, L. E. Marcucci and M. Viviani, nucl-th/0508048.
4. O. Benhar, contribution to these proceedings.
5. V. R. Pandharipande, I. Sick, and P. K. A. de Witt Huberts, Rev. Mod. Phys. **69**, 981 (1997).
6. W. H. Dickhoff and C. Barbieri, Prog. Part. Nucl. Phys. **52**, 377 (2004).
7. C. Ciofi degli Atti, S. Liuti, and S. Simula, Phys. Rev. C **41**, R2474 (1990).
8. O. Benhar, A. Fabrocini, S. Fantoni, and I. Sick, Nucl. Phys. **A579** 493 (1994).
9. H. Mütter and W. H. Dickhoff, Phys. Rev. C **49**, R17 (1994); H. Mütter, W. H. Dickhoff and A. Polls, Phys. Rev. C **51**, 3040 (1995).
10. Y. Dewulf, W. H. Dickhoff, D. Van Neck, E. R. Stoddard, and M. Waroquier Phys. Rev. Lett. **90**, 152501 (2003).
11. D. Rohe, *et al.*, Phys. Rev. Lett. **93**, 182501 (2004).
12. T. Frick, Kh. S. A. Hassaneen, D. Rohe and H. Mütter, Phys. Rev. C **70**, 024309 (2004).
13. D. Rohe, contribution to these proceedings.
14. T. Takaki, Phys. Rev. Lett. **62**, 395 (1989).
15. P. Demetriou, S. Boffi, C. Giusti, and F. D. Pacati, Nucl. Phys. **A625**, 513 (1997).
16. N. N. Nikolaev, *et al.*, Nucl. Phys. **A582**, 665 (1995).
17. A. Bianconi, S. Jeschonnek, N. N. Nikolaev, and B. G. Zakharov, Nucl. Phys. **A608**, 437 (1996); H. Morita, C. Ciofi degli Atti, and T. Treleani, Phys. Rev. C **60**, 034603 (1999).
18. S. Janssen, J. Ryckebusch, W. Van Nespen, and D. Debruyne, Nucl. Phys. **A672**, 285 (2000).
19. I. Sick, *Electron Nucleus Scattering*, eds. O. Benhar, A. Fabrocini, World Scientific, p. 445 (1997).
20. I. Sick, *et al.*, Jlab-Proposal E97-006, (1997).
21. D. Rohe, *Habilitationsschrift*, University of Basel, 2004 (unpublished).
22. C. Barbieri and L. Lapikás, Phys. Rev. C **70**, 054612 (2004).
23. C. Barbieri, D. Rohe, I. Sick and L. Lapikás, Phys. Lett. **B608**, 47 (2005).
24. O. Benhar, A. Fabrocini, and S. Fantoni Phys. Rev. Lett. **87** 052501 (2001).
25. T. de Forest, Jr., Nucl. Phys. **A392**, 232 (1983).
26. R. Schiavilla, D. S. Lewart, V. R. Pandharipande, S. C. Pieper, R. B. Wiringa, and S. Fantoni, Nucl. Phys. **A473**, 267 (1987).
27. H. de Vries, C. W. de Jager, and C. de Vries, Atomic Data and Nuclear Data Tables **36**, 495 (1987).
28. E. Amaldi, S. Fubini, G. Furlan, *Pion electroproduction*, Springer Tracts in Modern Physics **83**. Springer, Berlin (1979).
29. D. Drechsel, S. S. Kamalov and L. Tiator Nucl. Phys. **A645**, 145 (1999).
30. <http://www.kph.uni-mainz.de/MAID>.